Galactic Chemical Evolution in the Smallest Galaxies with Individual Stars

PI: Andrew Emerick, Carnegie Observatories and California Institute of Technology, Pasadena, CA

co-I: Alex Ji, Carnegie Observatories, Pasadena, CA

co-I: John Wise,

1 Introduction

Present-day stellar abundance patterns are tracers of the integrated history of galactic evolution. Ongoing and upcoming observations of detailed stellar abundance patterns, including SEGUE (**?**), RAVE (**?**), APOGEE (**?**), APOGEE-2 (**?**), GALAH (**?**), and the Pristine survey (**?**) have obtained an unprecedented number of stars with detailed, multi-element abundances in both the Milky Way and dwarf galaxies in the Local Group. This is in addition to the ongoing work obtaining detailed abundances of $\sim$100 or more stars by multiple groups (e.g. **?**, (need more!)) in low-mass dwarf galaxies in the Local Group. This allows us to directly probe the information-rich scatter in stellar abundance patterns across a range of environments and at low metallicities where the scatter is a more sensitive tracer of underlying galaxy evolution physics. These abundance patterns are the convolution of a galaxy's accretion and merger history, star formation history, internal dynamic structure, mixing timescales and efficiencies in the interstellar medium (ISM), stellar nucleosynthesis, and the effectiveness of stellar feedback in driving metal-rich galactic outflows. **last sentence**

The quality of these observations are rapidly outpacing our ability to simulate them, in large part because constructing such a model is complex. Since most metals are released through stellar winds, supernovae, or other similar energetic events, this model requires a detailed understanding of the role of stellar feedback in driving galactic evolution, a current open question in our field. In addition, models of galactic chemical evolution often lack an exact description for how metals mix within a multi-phase interstellar medium (ISM) and enrich future populations of stars.

motivate need to study high-z galaxy formation and evolution and connection to UFDs and low mass dwarfs

Since **?**, its been understood that the evolution of stellar abundance ratios as a function of metallicity (or, commonly, [Fe/H]) traces different chemical enrichment timescales. The most common example is the "knee" feature seen in plots of $[\alpha$/Fe] vs. [Fe/H] which represents the transition from core collapse supernova dominant enrichment (high $[\alpha$/Fe]) to significant contributions of Type Ia SNe (Fe, but no α). Similar trends can be expected for elements of different nucleosynthetic channels, such as the s-process in AGB stars, and elements with trends in yields as a function

of stellar mass. Each of these probe unique timescales in chemical evolution history. However, extracting information about these timescales from stellar abundances is complicated by the fact that the details of galaxy evolution – stellar feedback, star formation rate, IMF slope, and efficiencies of metal mixing in the ISM – drives significant scatter in elemental abundances ratios that makes interpreting any evolution quantitatively nearly impossible.

Doing this requires the type of simulations proposed here whereby the details of galaxy evolution are resolved to high-resolution, including star formation, stellar feedback, turbulent mixing, the formation of a multi-phase ISM, and a multi-element chemical evolution model that follows the abundances from individual stars. *These types of simulations have not yet been performed*. By following detailed chemical enrichment in the early Universe in our simulations, we will be able to unlock the connection between stellar abundances in Local Group ultrafaint dwarf galaxies and physics of galaxy evolution in the early Universe.

1.1 Key Scientific Questions and Goals

We provide a summary of the key scientific questions addressed by the simulations proposed in this project. These simulations are uniquely suited to address each of these issues, and the use of Stampede-2 is necessary to carry these out:

2 Proposed Computational Method and Model

Our simulations will be carried out using the publicly available cosmological adaptive mesh refinement (AMR) hydrodynamics and N-body code ENZO (**??**). ENZO is well-tested and has been used extensively in a variety of applications including studies of the ISM (**??**), the intergalactic medium (**??**), the first stars and galaxies (**?**), and the roles of stellar feedback in galactic evolution ().

Details about numerical methods in Enzo (hydro solver, gravity solver, load balancing, communication, AMR structure

We follow stellar radiation in five bands: HI, HeI, and HeII ionizing radiation, far ultraviolet (FUV), and Lyman-Werner (LW) radiation from all massive stars ($M_* > 8\ M_\odot$). Stellar properties are discussed further in Section **??**. Ionizing radiation is followed using the well-tested adaptive ray tracing radiative transfer method of (**?**) where photons packages are evolved as rays mapped to a HEALPIX grid, adaptively refined as they radiate from their source. To reduce computational expense – particularly in optically thin regions – we use source clusterings to allow rays to merge once they have travelled far from their source. FUV and LW radiation are both assumed to be optically thin. FUV radiation leads to photoelectric heating of dust grains in the ISM following **?** and the dust-to-gas ratio scaling in **?**. LW radiation is important for regulating cooling in metal-poor environments by dissociating the dominant coolant, H_2. We account for local self-shielding of LW radiation using the method from **?**. To dramatically reduce the computational expense of computing $1/r^2$ radiation for each star particle on each cell, we take advantage of the source

clustering tree to speed up this computation by an order of magnitude.

2.1 Initial Conditions

We build upon the work in (**????**), combined with the new star formation and stellar feedback model from (**?**). We will use the same set of cosmological initial conditions used in (**?**) to follow the formation of the first generation of dwarf galaxies. The simulation domain is a 1 Mpc (co-moving) box with a root-grid resolution of 256^3 and dark matter mass resolution of 1840 $M_\odot$. The simulation will be run with a maximum of 12 levels of additional refinement for a maximum resolution of 1 pc (co-moving) using a super-Lagrangian refinement scheme (**?**) to refine on baryon overdensities of $3 \times 2^{-0.2l}$, where l is the refinement level, dark matter overdensities of 3, and resolving the local Jeans length by at least 4 cells. In addition, we ensure that stellar feedback, metal enrichment, and metal mixing is well-resolved by forcing refinement in a 4-zone sphere around each star particle with active stellar feedback to at least a co-moving resolution of 4 pc. The simulation will begin at redshift z = 130 and we plan to run the simulation until a redshift of z = 7.

In Figure **??** we show the results of applying the methods discussed below to a low-resolution (61 co-moving pc, or 6.0 pc at z = 9.0) proof-of-concept test simulation with nested refinement on a single halo. The panels show projections of gas number density, temperature, [Fe/H], and HI ionization rate in the central region of the simulation box. Star particles are marked as black points. By this point in the simulation, a total mass of 5.0×10^5 $M_\odot$ of stars have formed, a majority of which is Pop II star formation, as the Pop III stars that do form (5.5×10^3 $M_\odot$) rapidly enrich this region to above the critial metallicity threshold. In addition, in Figure **??** we show the gas-phase distributions of

2.2 Star Formation

We outline the details of our physics models here, which includes some updates designed specifically for this project since their first development as described in detail in **?**. Star formation occurs stochastically in cells containing cold, dense gas ((co-moving or proper density?) cm^{-3}, $T < 500K$)) with a converging flow ($\nabla \cdot v < 0$) following a Schmidt law whereby the star formation rate density is given by $\rho_* = \epsilon_{\mathrm{ff}} \frac{\rho_g}{t_{\mathrm{ff}}}$, where ρ_g is the gas density, t_{ff} is the local gas free-fall time, and ϵ_{ff} is the efficiency per free-fall time, which we set to 1. In these cells, we stochastically form stars by computing the probability that 200 $M_\odot$ of gas will be turned into stars in a given time step. If this occurs, we random sample the stellar initial mass function, depositing individual star particles until at least 200 $M_\odot$ of stars form. We follow both Pop III star formation and Pop II star formation, with the former occurring only in cells with $Z < 10^{-4} Z_\odot$ and $f_{\mathrm{H}_2} > 5 \times 10^{-4}$ and the latter in metal enriched cells with $Z > 10^{-4} Z_\odot$. We adopt a **?**-like IMF for Pop III star formation above 100 $M_\odot$ with an exponential cutoff below this mass and a minimum and maximum particle

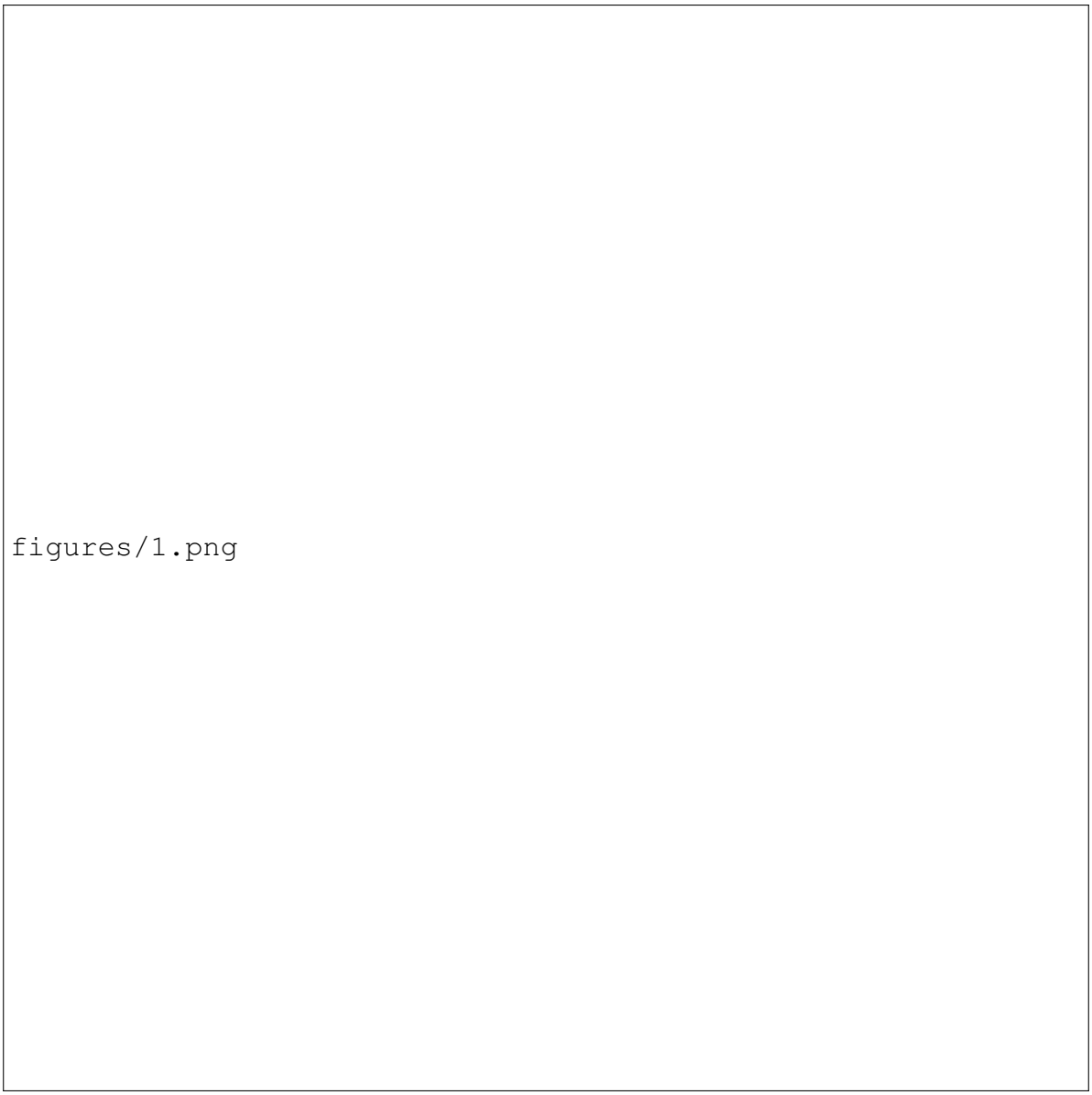

Figure 1: Projections of gas number density, temperature, [Fe/H], and HI ionization rate in the region of active star formation in a low-resolution test simulation run to z = 9.0. Individual star particles are overlaid as black points.

mass of 11 $M_\odot$ and maximum mass of 300 $M_\odot$. Pop II star formation follows a **?** IMF with a minimum and maximum mass of 0.08 $M_\odot$ and 100 $M_\odot$. Upon formation, the stellar abundances of each particle are written to file adopting the local gas abundances from which the stars form.

To reduce computational expense, we merge all Pop II star particles below 2 $M_\odot$ in each star forming cell into a single particle. These stars do not have significant feedback or metal enrichment on the timescale of these simulations ($\sim$ 1 Gyr), but still need to be followed as they are the key tracers of stellar abundances in present-day low mass dwarf galaxies.

2.3 Stellar Feedback

We follow a multi-channel stellar feedback prescription capturing stellar winds from massive stars and AGB stars, core collapse and Type Ia supernova, and ionizing radiation, Lyman-Werner radiation, and FUV radiation from massive stars. For both stellar winds and supernovae, mass and energy are deposited into 3-zone radius spherical regions around each star particle. We assume Pop III stars between 11 -40 $M_\odot$ and **140 - 260 $M_\odot$** and Pop II stars between 8 - 25 $M_\odot$ explode as core collapse supernovae at the end of their lives with 10^{51} erg of thermal energy. Stars above 25 M$\odot$ outside these ranges are assumed to direct collapse with no energy or mass ejection. We follow the H and He ionizing radiation for all stars above 8 $M_\odot$ using XXX for Pop III stars and the OSTAR2002 (**?**) grid of stellar spectra for Pop II stars. Ionizing radiation is followed using the adaptive ray-tracing radiative transfer method of CITE, which shows good scaling up to XXX sources. In addition, we track both the Lyman-Werner and FUV band radiation from these stars to follow H_2 dissociation and photoelectric heating on dust grains respectively. Radiation in these bands is assumed to be optically thin.

While stellar winds are potentially an important source of pre-SN feedback (**?**), their effects are sub-dominant to stellar ionizing radiation (cite). To reduce the computational expense of continually following fast ($\sim 10^3 \mathrm{kms}^{-1}$), hot ($T > 10^6$ K) gas throughout the lifetime of massive stars, we greatly reduce the velocities and energies of our stellar winds to just 10 km s^{-1} and a thermal energy equivalent to the surface temperature of the star. AGB star winds, for stars below 8 $M_\odot$ occur

2.4 Chemical Evolution

Since we follow individual star particles we can capture detailed, stochastic chemical evolution in our simulations – a significant improvement over commonly used IMF-averaged yield sets. We use the NuGrid set of stellar yields (**??**) to follow the mass and metallicity dependent stellar wind and core collapse supernova abundances of Pop II stars, including AGB winds. This is supplemented with abundances from Slemer et. al. *in prep.* for the stellar winds of stars above the upper mass limit of the NuGrid set, 25 $M_\odot$. For Pop III stars, we adopt the core-collapse SNe metal-free yields from **?** for stars between 13 $M_\odot$ and 40 $M_\odot$ and the PISN yields of **?** for stars between 60 $M_\odot$

and 130 $M_\odot$. Yields for Pop III stars that explode and release metals at the end of their life that are outside these mass ranges adopt the abundances of the closest grid point, scaled by mass. For Type Ia supernovae, we adopt the yields from **?**.

We plan to follow the metal abundances of 8 elements from each of these sources, C, N, O, Mg, Ca, Fe, Sr, and Ba, in addition to the total metallicity and separate fields tracking the fractional contribution of Pop III stars, Pop II core collapse SN, Type Ia SN, and AGB stars to the total metallicity. This gives us a total of 13 metal tracer fields on top of the 9 non-equillibrium chemistry fields. These elements were chosen carefully to maximize both the ability to resolve distinct nucleosynthetic channels and stellar enrichment timescales and usefulness for comparisons to observations, while minimizing the significant additional memory overhead for each additional field.[1] O, Mg, and Ca are all produced in significant amounts in core collapse SN, and show a noticeable evolution with supernova progenitor mass, tracing short-timescale (10 Myr) chemical evolution. Fe is produced in both core collapse and Type Ia supernova, and the relative abundances of O, Mg, and Ca to Fe traces the evolution between these two yields sources on timescales of 100 Myr to 1 Gyr.[2]. N, Sr, and Ba all trace s-process enrichment in low-mass AGB stars on timescales of 100 Myr to 1 Gyr, with N and Ba tracing the most massive (4-8 $M_\odot$) AGB stars and Sr the less massive ($< 4\ M_\odot$). C also has significant production in low-mass AGB stars, but is also produced in core collapse supernova. The C to Fe ratio is an important tracer of early Pop III enrichment. All of these elements are readily observed in a majority of low to medium stellar spectra, with the exception of O. However, O is the most abundant metal species and is used as an important tracer of gas-phase abundances.

Finally, the origin of r-process enrichment is still highly debated (e.g.). Given that the origin of r-process enrichment is uncertain and that possible sources of enrichment are rare and therefore strongly subject to stochastic variations in our simulation volume, we do not include an explicit channel for either core collapse SNe or NS-NS merger r-process enrichment. However, as XX - XX $M_\odot$ stars are expected to be possible sources of r-process enrichment, we follow their metal enrichment as a separate tracer field that can be used to post-process individual r-process abundances given models for their yields and scaling their expected frequency per XX - XX $M_\odot$ supernovae in the simulation. While this does not directly account for NS-NS r-process enrichment, this will test what – if any – r-process feautures in observed abundance patterns can be explained by CCSNe alone, and what features likely require an additional source of enrichment.

[1] Assuming a typical simulation has $\sim 10^8$ zones, each tracer field incurs a *minimum* additional memory requirement of 800 MB (64-bits $\times$ 10^8). This represents the on-disk memory requirements for each field in the output data files. In practice, however, the actual run-time overhead is much larger as this does not include the requirements for ghost zones around each grid and additional space in communication buffers. The minimum memory requirement for all 13+9 species fields is 16.8 GB.

[2] Additional Type Ia elemental yields (e.g. Ni and Mn) can readily be post-processed using the Type Ia tracer field.

Figure 2: Test

3 Proposed Computational Resources

We propose to carry out a single simulation

The original simulations of **?** utilized $\sim$250,000 CPU hours running on 512 cores on a NASA machine. This run time – if used on the Stampede 2 SKX nodes – translates to 5371 SU (250,000/512 $|times$ 11, where 11 is the number of 48-core nodes needed to have at least 512 total cores) if run on Stampede-2. Ho

Run	Parameter 1	Parameter 2	#cores	#Nodes	Wall Time (days)	**SUs**
					Total	

4 Project Team Qualifications

5 Management

5.1 Summary

5.2 Local Computing Environment

5.3 Other Supercomputing Support